LETTERS

Strong dispersive coupling of a high-finesse cavity to a micromechanical membrane

J. D. Thompson[1], B. M. Zwickl[1], A. M. Jayich[1], Florian Marquardt[2], S. M. Girvin[1,3] & J. G. E. Harris[1,3]

Macroscopic mechanical objects and electromagnetic degrees of freedom can couple to each other through radiation pressure. Optomechanical systems in which this coupling is sufficiently strong are predicted to show quantum effects and are a topic of considerable interest. Devices in this regime would offer new types of control over the quantum state of both light and matter[1–4], and would provide a new arena in which to explore the boundary between quantum and classical physics[5–7]. Experiments so far have achieved sufficient optomechanical coupling to laser-cool mechanical devices[8–12], but have not yet reached the quantum regime. The outstanding technical challenge in this field is integrating sensitive micromechanical elements (which must be small, light and flexible) into high-finesse cavities (which are typically rigid and massive) without compromising the mechanical or optical properties of either. A second, and more fundamental, challenge is to read out the mechanical element's energy eigenstate. Displacement measurements (no matter how sensitive) cannot determine an oscillator's energy eigenstate[13], and measurements coupling to quantities other than displacement[14–16] have been difficult to realize in practice. Here we present an optomechanical system that has the potential to resolve both of these challenges. We demonstrate a cavity which is detuned by the motion of a 50-nm-thick dielectric membrane placed between two macroscopic, rigid, high-finesse mirrors. This approach segregates optical and mechanical functionality to physically distinct structures and avoids compromising either. It also allows for direct measurement of the square of the membrane's displacement, and thus in principle the membrane's energy eigenstate. We estimate that it should be practical to use this scheme to observe quantum jumps of a mechanical system, an important goal in the field of quantum measurement.

Experiments and theoretical proposals aiming to study quantum aspects of the interaction between optical cavities and mechanical objects have focused on cavities in which one of the cavity's mirrors is free to move (for example, in response to radiation pressure exerted by light in the cavity). A schematic of such a setup is shown in Fig. 1a. Although quite simple, Fig. 1a captures the relevant features of nearly all optomechanical systems described in the literature, including cavities with 'folded' geometries, cavities in which multiple mirrors are free to move[5], and whispering gallery mode resonators[14] in which light is confined to a waveguide. All these approaches share two important features. First, the optical cavity's detuning is proportional to the displacement of a mechanical degree of freedom (that is, mirror displacement or waveguide elongation). Second, a single device must provide both optical confinement and mechanical pliability.

In these systems, optomechanical coupling can be strong enough to laser-cool their brownian motion by a factor of 400 via passive cooling[13]. But the coupling has been insufficient to observe quantum
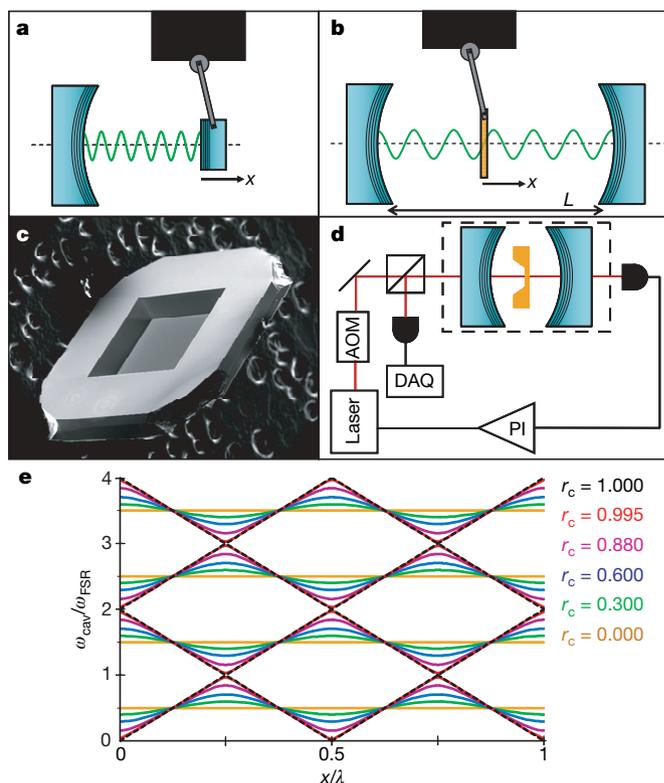

Figure 1 | Schematic of the dispersive optomechanical set-up.
a, Conceptual illustration of 'reflective' optomechanical coupling. The cavity mode (green) is defined by reflective surfaces, one of which is free to move. The cavity detuning is proportional to the displacement x. **b**, Conceptual illustration of the 'dispersive' optomechanical coupling used in this work. The cavity is defined by rigid mirrors. The only mechanical degree of freedom is that of a thin dielectric membrane (orange) in the cavity mode (green). The cavity detuning is periodic in the displacement x. The total cavity length is $L = 6.7$ cm. **c**, Photograph of a SiN membrane (1 mm $\times 1$ mm $\times 50$ nm) on a silicon chip. **d**, Schematic of the optical and vacuum setup. The vacuum chamber (dotted line) is ion-pumped to $\sim 10^{-6}$ torr. The membrane chip is shown in orange. The optical path includes an AOM for switching the laser beam on and off, and a proportional-integral (PI) servo loop for locking the laser to the cavity. The reflected laser power is recorded by a data acquisition system (DAQ). **e**, Calculation of the cavity frequency $\omega_{\mathrm{cav}}(x)$ in units of $\omega_{\mathrm{FSR}} = \pi c/L$. Each curve corresponds to a different value of the membrane reflectivity r_{c}. Extrema in $\omega_{\mathrm{cav}}(x)$ occur when the membrane is at a node (or antinode) of the cavity mode. Positive (negative) slope of $\omega_{\mathrm{cav}}(x)$ indicates the light energy is stored predominantly in the right (left) half of the cavity, with radiation pressure force acting to the left (right).

[1]Department of Physics, Yale University, 217 Prospect Street, New Haven, Connecticut, 06520, USA. [2]Physics Department, Center for NanoScience, and Arnold Sommerfeld Center for Theoretical Physics, Ludwig Maximilians University, Theresienstrasse 37, 80333, Munich, Germany. [3]Department of Applied Physics, Yale University, 15 Prospect Street, New Haven, Connecticut 06520, USA.

effects such as quantum fluctuations (shot noise) of the radiation pressure. To illustrate the connection between observing quantum effects and the properties of the devices in Fig. 1a we consider a figure of merit R, the ratio between the force power spectral densities of radiation pressure shot noise ($S_F^{(\gamma)}$) and thermal fluctuations ($S_F^{(T)}$): $R \equiv S_F^{(\gamma)}/S_F^{(T)} = 16\hbar P_{in} Q F^2 / \lambda c\pi k_B T m\omega_m$. Here P_{in} and λ are the laser power and wavelength incident on the cavity; F is the cavity finesse; Q, m and ω_m are the mechanical element's quality factor, motional mass and resonant frequency; and T is the temperature of the thermal bath. This expression highlights the importance of achieving both good optical properties (high F) and good mechanical properties (high Q; small m, spring constant k).

Simultaneously achieving good mechanical and optical properties has been the main technical barrier to realizing quantum optomechanical systems. In large part this is because high-finesse mirrors are not easily integrated into micromachined devices. These mirrors are typically SiO_2/Ta_2O_5 multilayers which are mechanically lossy[17] (limiting Q); they must also be $\sim 2\,\mu m$ thick and $\sim 30\,\mu m$ in diameter to avoid transmission and diffraction losses[18,19], setting lower limits on m and k; and the mirror's cleanliness and flatness must be maintained during micromachining. As a result most experiments (including those using whispering gallery mode resonators) reach a compromise between high-quality optical or mechanical properties.

Figure 1b shows a cavity layout that differs from Fig. 1a and is the focus of this paper. The cavity is a standard high-finesse Fabry–Perot which in our laboratory is formed between two macroscopic, rigid, commercial mirrors mounted to a rigid spacer. These mirrors are assumed to be fixed. The mechanically compliant element is a thin dielectric membrane placed at the waist of the cavity mode. We use a commercial SiN membrane 1 mm square by 50 nm thick. The membrane is supported by a silicon frame (a typical device is shown in Fig. 1c). The cavity is excited by a laser with $\lambda = 1,064$ nm. The beam path is shown in Fig. 1d.

Unlike the cavities illustrated in Fig. 1a, the coupling between the membrane and the optical cavity in Fig. 1b depends on where the membrane is placed relative to the nodes of the cavity mode (shown in green in Fig. 1b). This results in a cavity detuning $\omega_{cav}(x)$ which is periodic in the membrane displacement x, in analogy with the dispersive coupling in some atom-cavity experiments[20,21]. A one-dimensional calculation gives $\omega_{cav}(x) = (c/L)\cos^{-1}[|r_c|\cos(4\pi x/\lambda)]$ where L is the cavity length and r_c is the membrane's (field) reflectivity. Figure 1e shows a plot of $\omega_{cav}(x)$ for various values of r_c. This geometry is discussed in ref. 22, although not its connection to the fabrication and quantum non-demolition issues discussed here.

The optical force on the membrane is proportional to $\partial\omega_{cav}/\partial x \propto |r_c|$, so using a membrane with modest r_c does not substantially reduce the optomechanical coupling. Thus our approach removes the need to integrate good mirrors into good mechanical devices. We have made use of the fact that the cavity mirrors set F, and the mechanical element's reflectivity only determines the fraction of intracavity photons that transfer momentum to the membrane. Our approach also relaxes the constraint on the mechanical element's thickness, although not on its lateral size.

For this 'membrane-in-the-middle' approach to work, the membrane must not diminish F through absorption or scatter, or by coupling light into lower-F modes. Figure 2a shows cavity ringdown measurements with the membrane removed (blue), and with the membrane inserted at an antinode (green) or node (red) of the intracavity field. Fitting the empty cavity data gives $F_0 = 16,100$. With the membrane at an antinode F drops to $F_{AN} = 6,940$, implying $\mathrm{Im}(n_{SiN}) = 1.6 \times 10^{-4}$ (n_{SiN} is the membrane's refractive index), consistent with tabulated optical properties[23] of SiN. But when the membrane is placed at a node, the finesse is $F_N = 15,200$, equal to F_0 to within the repeatability of the measurement ($\sim 10\%$).

Figure 2a thus highlights an additional important advantage of the 'membrane-in-the-middle' geometry. It allows us to use a membrane much thinner than λ and to position it at a cavity node, greatly reducing the overlap of the membrane with the optical field and making the membrane's already small optical losses essentially irrelevant. This is important both for maintaining high F and ensuring the mechanical device is not heated by absorption of light. By contrast, a cantilever-mounted mirror as in Fig. 1a must overlap with several antinodes[18]. A similar suppression is used in blue-detuned optical lattices where atoms are trapped at the optical field nodes and experience greatly reduced scattering[24]. Straightforward calculations show that with the measured SiN optical loss, commercially available end mirrors could allow $F > 5 \times 10^5$ if the membrane is placed at a node.

Figure 2b shows the transmission through the cavity as function of laser frequency and x. The bright bands correspond to cavity
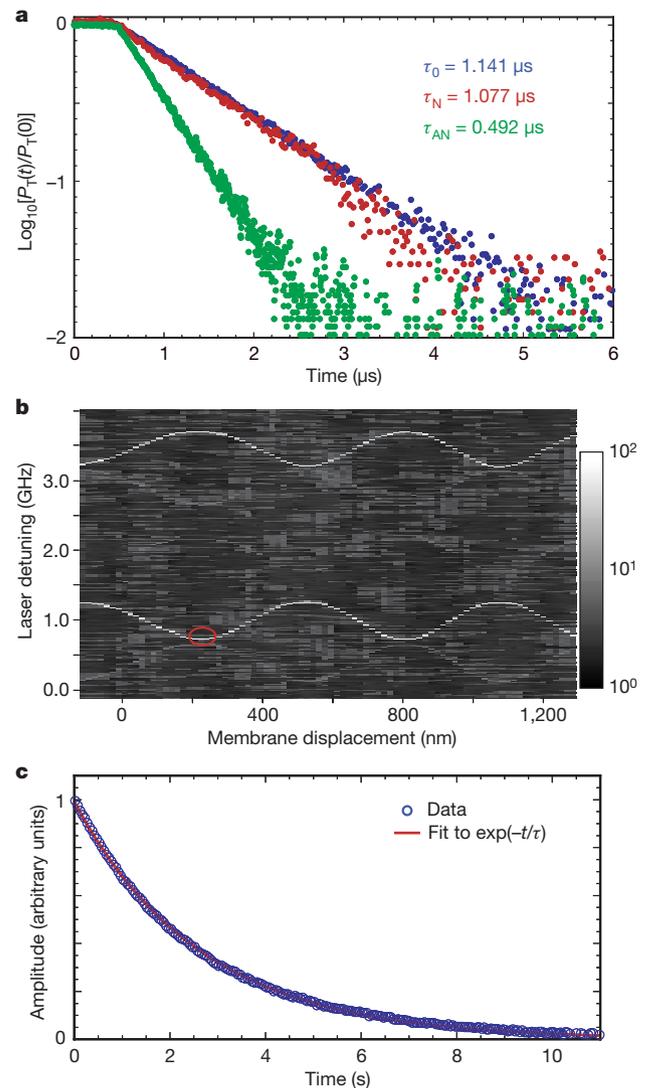

Figure 2 | Optical and mechanical characterization of the cavity.
a, Ringdown measurements of the cavity with the membrane removed (blue), and with it placed at a cavity node (red) or at an antinode (green). The transmitted power P_T is plotted as a function of time. The laser is switched off at 400 ns. An offset has been subtracted from the data. The exponential time constants (τ_0, τ_N and τ_{AN}) fitted to the data correspond to cavity finesses $F_0 = 16,100$, $F_N = 15,200$ and $F_{AN} = 6,940$. **b**, Logarithmic greyscale plot of the cavity transmission versus laser detuning and membrane position. The two brightest curves correspond to the cavity's TEM_{00} mode. Fitting the data gives the membrane reflectivity $r_c = 0.42$ (see Fig. 1e). The fainter curves are higher-order transverse modes. **c**, Ringdown measurement of the membrane's lowest mechanical resonance. The fit gives a ringdown time $\tau = 2.67$ s, corresponding to $Q = \omega_m\tau/2 = 1.1 \times 10^6$.
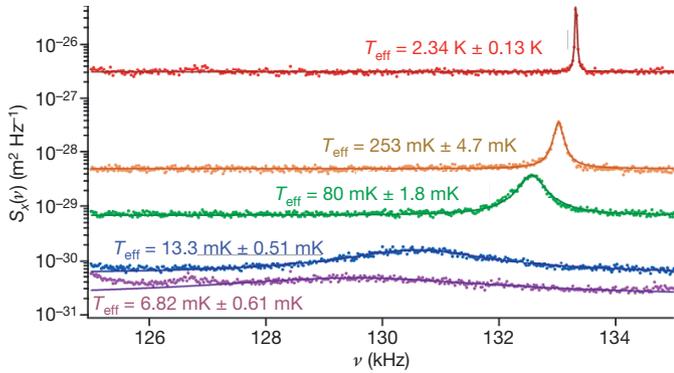
Figure 3 | Passive laser cooling of the membrane. The power spectral density S_x of the membrane's undriven motion at different values of the laser detuning (from top to bottom: 4.84, 2.18, 1.66, 1.00 and 0.71 cavity linewidths) and an incident optical power $P_{in} = 114\,\mu W$ (except for the uppermost curve for which $P_{in} = 359\,\mu W$). Solid lines are fits to a damped driven oscillator model. The effective temperature T_{eff} of the membrane is determined from Q_{eff} and is indicated on the figure (the quoted error is the statistical error in fitting Q_{eff}, as determined from the fit residuals). A broad feature partially visible at the left of the lowest two data sets is due to electrical noise and was excluded from the fits. The noise floor is set by stationary voltage noise at the detector. The noise floor differs in the curves because of the detuning dependence of the volts-to-metres conversion.

resonances. Fitting the data gives $r_c = 0.42$, consistent with the membrane thickness and $Re(n_{SiN}) = 2.2$.

Figure 2c shows the mechanical ringdown of the membrane's lowest flexural resonance at $\omega_m = 2\pi \times 134\,kHz$. From ω_m and m (calculated from the membrane dimensions to be 4×10^{-8} g) we find the spring constant $k = 28\,N\,m^{-1}$. Fitting the data in Fig. 2c gives $Q = 1.1 \times 10^6$.

For small oscillation amplitudes the membrane is well described as a harmonic oscillator and $\omega_{cav}(x)$ is linear to lowest order in x (except at an extremum of $\omega_{cav}(x)$). Thus this device can mimic the traditional optomechanical systems illustrated in Fig. 1a, but without the technical challenge of integrating mirrors into cantilevers.

To illustrate this point, we use the mechanism described in refs 9–12 to laser-cool the membrane's brownian motion. Figure 3 shows the power spectral density of the membrane's undriven motion $S_x(\nu)$ when the laser is slightly red-detuned from the cavity resonance. The membrane's motion is monitored by means of the light reflected from the cavity while the laser detuning and P_{in} are varied. As described elsewhere[9–12], the radiation pressure exerted by the red-detuned laser damps the membrane's brownian motion.

We extract the membrane's effective temperature T_{eff} from the data in Fig. 3 in two ways: $T_{eff}^{(x)} = m\omega_m^2\langle x^2\rangle/k_B$ or $T_{eff}^{(Q)} = TQ_{eff}/Q$ where $\langle x^2\rangle = \int S_x(\nu)d\nu$ and the effective Q factor Q_{eff} is found by fitting each curve. The values of $T_{eff}^{(x)}$ and $T_{eff}^{(Q)}$ agree to within a factor of ~2, with $T_{eff}^{(x)}$ systematically less than $T_{eff}^{(Q)}$. Because $T_{eff}^{(x)}$ may be affected by small errors in the absolute calibration of x, we cite $T_{eff}^{(Q)}$ in Fig. 3.

The lowest temperature achieved in Fig. 3 is 6.82 mK, a factor of 4.4×10^4 below the starting temperature of 294 K. This is a cooling ratio more than 100 times greater than has been achieved previously with passive laser cooling of mechanical devices[11]. It is made possible by the geometry of this system, which allows us to combine high-F cavities with high-Q, low-k mechanical oscillators.

The laser cooling in Fig. 3 was obtained by positioning the membrane so that $\omega_{cav}(x)$ is proportional to x. However, if the membrane is positioned at an extremum of ω_{cav} (red circle in Fig. 2b), then to lowest order $\omega_{cav}(x) \propto x^2$. In this case, light leaving the cavity carries information only about x^2. The ability to realize a direct x^2-measurement is a fundamental difference between our approach and previous work because it can be used as a quantum non-demolition readout of the membrane's phonon number eigenstate[13].

To see this we note that the Hamiltonian of the optomechanical system is $\hat{H} = \hbar\omega_{cav}(\hat{x})\hat{a}^\dagger\hat{a} + \hbar\omega_m\hat{b}^\dagger\hat{b}$ where $\hat{a}$ and $\hat{b}$ are the lowering operators for the optical and mechanical modes, $\hat{x} = x_m(\hat{b}^\dagger + \hat{b})$, and $x_m = \sqrt{\hbar/2m\omega_m}$. With the membrane at an extremum of ω_{cav} (for example, $x = 0$), we can expand $\hat{H} \approx \hbar(\omega_{cav}(0) + \frac{1}{2}\omega''_{cav}(0)x_m^2(\hat{b}^\dagger + \hat{b})^2)\hat{a}^\dagger\hat{a} + \hbar\omega_m\hat{b}^\dagger\hat{b}$ where $\omega''_{cav} = \partial^2\omega_{cav}/\partial x^2$. In the rotating wave approximation (valid when $\pi c/LF \ll \omega_m$)[25], this becomes $\hat{H} \approx \hbar(\omega_{cav}(0) + \omega''_{cav}(0)x_m^2(\hat{b}^\dagger\hat{b} + \frac{1}{2}))\hat{a}^\dagger\hat{a} + \hbar\omega_m\hat{b}^\dagger\hat{b}$. Thus, within this approximation, $[\hat{H}, \hat{b}^\dagger\hat{b}] = 0$, and so the membrane's phonon number can be measured without back action. In principle $\hat{b}^\dagger\hat{b}$ can be read out by monitoring the optical cavity: it experiences a detuning-per-phonon $\Delta\omega_{cav} = x_m^2\omega''_{cav}(0)$ which can be monitored with a Pound–Drever–Hall circuit.

The presence of extrema in $\omega_{cav}(x)$ thus provides an optomechanical coupling of the form required for quantum non-demolition measurements of the membrane's phonon number. Whether such a measurement can be used to observe a quantum jump of the membrane depends on whether $\Delta\omega_{cav} = (16\pi^2cx_m^2/L\lambda^2)\sqrt{2(1 - r_c)}$ can be resolved in the lifetime of a phonon number state. The shot-noise-limited sensitivity of an ideal Pound–Drever–Hall detector is[26] $S_{\omega_{cav}} = \pi^3\hbar c^3/16F^2L^2\lambda P_{in}$, and the (power) signal-to-noise ratio for resolving a jump from the nth phonon state is $\Sigma^{(n)} = \tau_{tot}^{(n)}\Delta\omega_{cav}^2/S_{\omega_{cav}}$. For realistic parameters we find that the lifetime of the nth phonon state $\tau_{tot}^{(n)}$ is primarily limited by thermal excitations, with small corrections due to the rotating wave approximation and imperfect positioning of the membrane at $x = 0$. The relevant calculation is in the Supplementary Information.

For our estimates we assume that $T = 300$ mK, that the membrane is laser-cooled to its ground state[25], and that the cooling laser is then shut off. We calculate $\Sigma^{(0)}$, the signal-to-noise ratio for observing the quantum jump of the membrane out of its ground state. Table 1 shows two sets of experimental parameters giving $\Sigma^{(0)} \approx 1$. The parameters in Table 1, although challenging, seem feasible. We have measured $Q = 1.2 \times 10^7$ for these membranes at $T = 300$ mK, and have cryogenically cooled the brownian motion of similar devices[27] to 300 mK. The x^2-measurement can be realized with the membrane at a node, so $F > 3 \times 10^5$ should be possible. With the membrane at a node, we assume that P_{in} of a few microwatts would not lead to excessive heating. The mass $m = 5 \times 10^{-11}$ g is the motional mass of a membrane 50 nm thick and 40 μm in diameter. Remarkably, patterning such a membrane can lead to high r_c (ref. 28) and may allow for $r_c > 0.999$ (O. Solgaard, personal communication). The required picometre-scale placement of the membrane is within the stability and resolution of cryogenic positioning systems[29]. According to the standard theory of radiation pressure cooling[25,30], the parameters in Table 1 should allow laser cooling to the membrane's ground state ($n < 0.1$) using P_{in} as low as 0.1 nW. Experiments with higher-F mirrors and cryogenic pre-cooling are under way in our laboratory.

The new type of optomechanical coupling that we have developed resolves a number of the outstanding technical issues faced by previous approaches. It offers the new feature of allowing a sensitive

Table 1 | Parameters for observing a membrane's quantum jumps

Q	T (K)	F	P_{in} (μW)	m (pg)	$\omega_m/2\pi$ (Hz)	r_c	x_0 (pm)	λ (nm)	$\tau^{(0)}$ (ms)	$\Sigma^{(0)}$
1.2×10^7	0.3	3×10^5	10	50	10^5	0.999	0.5	532	0.3	1.0
1.2×10^7	0.3	6×10^5	1	50	10^5	0.9999	0.5	532	0.3	4.0

Two sets of experimental parameters that would allow observation of an individual quantum jump from the membrane's ground state to its first excited state.

x^2-measurement which should make it possible to measure the quantum jumps of micrometre-scale mechanical oscillators. This approach should make it straightforward to couple multiple mechanical devices to a single cavity mode. Stacking multiple chips like the one in Fig. 1c would give a self-aligned array of membranes which could be placed inside a cavity. Such a complex optomechanical system would be particularly interesting for studying entanglement between the membranes[4] or using one membrane to provide a quantum non-demolition readout of another.

METHODS SUMMARY

The optical cavity is formed between two commercial mirrors rigidly attached to an Invar spacer. The SiN membrane is mounted inside the cavity on a stage which allows us to adjust *in situ* the membrane's tilt relative to the cavity axis and its position along the cavity axis. The stage also includes a piezoelectric element which allows us to excite the lowest several vibrational modes of the membrane.

The cavity is illuminated by a continuous-wave Nd:YAG laser. The beam path includes an acousto-optic modulator (AOM) which is used to chop the laser beam in order to perform the cavity ringdown measurements in Fig. 2a.

To measure Q the membrane's lowest vibrational mode mode was excited by means of the piezoelectric drive. The drive was then abruptly switched off and the membrane's ringdown was monitored, as shown in Fig. 2c. For these measurements we used a laser with $\lambda = 1,550$ nm. At this wavelength, $F \approx 1$, ensuring that the laser light does not affect the membrane's mechanical properties. Measurements of Q at cryogenic temperatures were carried out in a ^{3}He refrigerator using a fibre-optic interferometer and $\lambda = 1,550$ nm laser light.

The calibration of the brownian motion signals in Fig. 3 is somewhat more complicated than for optomechanical systems using the 'usual' geometry. This is because the cavity detuning (shown in Fig. 1e) depends on the membrane reflectivity as well as its position relative to a node in the optical field. Our calibration procedure involves measuring the photodiode signal produced by a frequency modulation of the laser (equivalent to modulation of the cavity detuning or modulation of the membrane displacement) and then calibrating the cavity detuning in terms of the membrane displacement. This requires several intermediate steps described in the online Methods.

Full Methods and any associated references are available in the online version of the paper at www.nature.com/nature.

1. Fabre, C. *et al.* Quantum-noise reduction using a cavity with a movable mirror. *Phys. Rev. A.* **49**, 1337–1343 (1994).
2. Giovannetti, V., Mancini, S. & Tombesi, P. Radiation pressure induced Einstein–Podolsky–Rosen paradox. *Europhys. Lett.* **54**, 559–565 (2001).
3. Vitali, D. *et al.* Optomechanical entanglement between a movable mirror and a cavity field. *Phys. Rev. Lett.* **98**, 030405 (2007).
4. Pinard, M. *et al.* Entangling movable mirrors in a double-cavity system. *Europhys. Lett.* **72**, 747–753 (2005).
5. Bose, S., Jacobs, K. & Knight, P. L. Scheme to probe the decoherence of a macroscopic object. *Phys. Rev. A.* **59**, 3204–3210 (1999).
6. Marshall, W., Simon, C., Penrose, R. & Bouwmeester, D. Towards quantum superpositions of a mirror. *Phys. Rev. Lett.* **91**, 130401 (2003).
7. Fereira, A., Geirreiro, A. & Vedral, V. Macroscopic thermal entanglement due to radiation pressure. *Phys. Rev. Lett.* **96**, 060407 (2006).
8. Höhberger, C. & Karrai, K. Cavity cooling of a microlever. *Nature* **432**, 1002–1005 (2004).
9. Gigan, S. *et al.* Self cooling of a micromirror by radiation pressure. *Nature* **444**, 67–70 (2006).
10. Arcizet, O., Cohadon, P.-F., Briant, T., Pinard, M. & Heidmann, A. Radiation-pressure cooling and optomechanical instability of a micromirror. *Nature* **444**, 71–74 (2006).
11. Corbitt, T. *et al.* An all-optical trap for a gram-scale mirror. *Phys. Rev. Lett.* **98**, 150802 (2007).
12. Schliesser, A., Del'Haye, P., Nooshi, N., Vahala, K. J. & Kippenberg, T. J. Radiation pressure cooling of a micromechanical oscillator using dynamical backaction. *Phys. Rev. Lett.* **97**, 243905 (2006).
13. Braginsky, V. B., Vorontsov, Y. I. & Thorne, K. S. Quantum nondemolition measurements. *Science* **209**, 547–557 (1980).
14. Santamore, D. H., Doherty, A. C. & Cross, M. C. Quantum nondemolition measurements of Fock states of mesoscopic mechanical oscillators. *Phys. Rev. B* **70**, 144301 (2004).
15. Martin, I. & Zurek, W. H. Measurement of energy eigenstates by a slow detector. *Phys. Rev. Lett.* **98**, 120401 (2007).
16. Jacobs, K., Lougovski, P. & Blencowe, M. Continuous measurement of the energy eigenstates of a nanomechanical resonator without a nondemolition probe. *Phys. Rev. Lett.* **98**, 147201 (2007).
17. Harry, G. M. *et al.* Thermal noise in interferometric gravitational wave detectors due to dielectric optical coatings. *Class. Quantum Grav.* **19**, 897–917 (2002).
18. Hood, C. J., Kimble, H. J. & Ye, J. Characterization of high-finesse mirrors: Loss, phase shifts, and mode structure in an optical cavity. *Phys. Rev. A.* **64**, 033804 (1999).
19. Kleckner, D. *et al.* High finesse opto-mechanical cavity with a movable thirty-micron-size mirror. *Phys. Rev. Lett.* **96**, 173901 (2006).
20. Brune, M., Haroche, S., Lefevre, V., Raimond, J. M. & Zagury, N. Quantum nondemolition measurement of small photon numbers by Rydberg-atom phase-sensitive detection. *Phys. Rev. Lett.* **65**, 976–979 (1990).
21. Wallraff, A. *et al.* Strong coupling of a single photon to a superconducting qubit using circuit quantum electrodynamics. *Nature* **431**, 162–167 (2004).
22. Meystre, P., Wright, E. M., McCullen, J. D. & Vignes, E. Theory of radiation-pressure-driven interferometers. *J. Opt. Soc. Am. B* **2**, 1830–1840 (1985).
23. Poenar, D. P. & Wolffenbuttel, R. F. Optical properties of thin-film silicon-compatible materials. *Appl. Opt.* **36**, 5122–5128 (1997).
24. Müller-Seydlitz, T. *et al.* Atoms in the lowest motional band of a three-dimensional optical lattice. *Phys. Rev. Lett.* **78**, 1038–1041 (1997).
25. Marquardt, F., Chen, J. P., Clerk, A. A. & Girvin, S. M. Quantum theory of cavity-assisted sideband cooling of mechanical motion. *Phys. Rev. Lett.* **99**, 093902 (2007).
26. Black, E. D. An introduction to Pound−Drever−Hall laser frequency stabilization. *Am. J. Phys.* **69**, 79–87 (2001).
27. Bleszynski, A. C., Shanks, W. E. & Harris, J. G. E. Noise thermometry and electron thermometry of a sample-on-cantilever system below 1 Kelvin. *Appl. Phys. Lett.* **92**, 013123 (2008).
28. Kilic, O. *et al.* Photonic crystal slabs demonstrating strong broadband supression of transmission in the presence of disorders. *Opt. Lett.* **29**, 2782–2784 (2004).
29. Stipe, B. C., Rezaei, M. A. & Ho, W. A variable-temperature scanning tunneling microscope capable of single-molecule vibrational spectroscopy. *Rev. Sci. Instrum.* **70**, 137–143 (1999).
30. Wilson-Rae, I., Nooshi, N., Zwerger, W. & Kippenberg, T. J. Theory of ground state cooling of a mechanical oscillator using dynamical backaction. *Phys. Rev. Lett.* **99**, 093901 (2007).

METHODS

The optical cavity is formed by two mirrors with specified (power) reflectivity $R = 0.9998$ at $\lambda = 1,064$ nm (consistent with the empty-cavity ringdown data in Fig. 2a) and radius of curvature $r = 10$ cm (Advanced Thin Films). The two mirrors are attached to opposite ends of a cylindrical Invar spacer 6.7 cm long. A hole is drilled through the Invar along the cavity axis to accommodate the cavity mode, and a second hole is drilled perpendicular to the cavity axis. The membrane is introduced into the cavity mode through the second hole.

The membrane chip is mounted on a piezoelectric disk with ~300 kHz of bandwidth and a maximum displacement of a few nanometres. This disk is used to excite the membrane's mechanical resonances. The disk is mounted on a larger piezoelectric stack which controls the membrane's d.c. displacement over a 1-µm span along the cavity axis (used, for example, for the data in Fig. 2b). The piezo stack is controlled in an open loop, but is stable enough to maintain the membrane's position relative to a cavity node to within a few nanometres over several hours (for example, for the data taken in Fig. 3). This piezoelectric stack is in turn mounted on a commercial motor-driven tilt stage (Thor Labs) which allows *in situ* alignment of the membrane's tilt relative to the cavity axis. In practice, we find alignment to ±4 mrad is required to maintain the cavity finesse.

The TEM$_{00}$ cavity mode has a $1/e^2$ diameter of 90 µm at the membrane, and so fits comfortably within the 1 mm × 1 mm membrane.

The laser light incident on the cavity is generated by a continuous-wave $\lambda = 1,064$ nm Nd:YAG laser (Innolight). The laser beam passes through an AOM which can be used to switch off the laser in roughly 30 ns.

To measure the cavity ringdown time, the laser frequency is swept across the cavity line. A photodiode monitoring the transmitted power triggers the AOM when its signal rises above a predetermined level, cutting off the laser light incident on the cavity. The same photodiode records the cavity ringdown after the laser is switched off (for example, the data shown in Fig. 2a).

To measure the membrane's quality factor Q, we drive the membrane chip using the small piezoelectric disk at the membrane's lowest mechanical resonance ($\omega_{\mathrm{m}} \approx 2\pi \times 1.34 \times 10^5$ Hz). For these measurements, the 1,064-nm laser is kept off, and the membrane is monitored using a $\lambda = 1,550$ nm diode laser. At this wavelength, the cavity finesse is ~1, ensuring that radiation pressure effects do not modify the membrane's mechanical properties.

The same electronic signal used to drive the piezoelectric disk serves as the reference for a lock-in measurement of the transmitted 1,550-nm intensity. After the membrane amplitude has reached its steady state, the signal is disconnected from the piezo and the lock-in monitors the component of the transmitted light at ω_0. This signal is proportional to the amplitude of the membrane motion and is plotted in Fig. 2c. Note that the optical ringdown (Fig. 2a) monitors the power in the optical field, whereas the mechanical ringdown monitors the membrane amplitude.

All the data presented here were taken on the membrane's lowest mechanical mode. However, we have also measured the frequencies of the lowest 30 mechanical modes and found they agree with the spectrum of modes for a taut square drumhead to better than 0.1%. This allows us to conclude that the membrane is well modelled as a taut square drumhead. For such an object, the motional mass of any mode is given by one-quarter of the physical mass.

To measure the membrane displacement, we use a photodiode to monitor the intensity of light reflected from the cavity. The conversion of the photodiode current to the membrane displacement depends on the laser power P, the detuning from the cavity resonance Δ, and the position x_0 of the membrane relative to a cavity node, so a separate calibration is needed when any of these quantities is changed (for example, for each curve in Fig. 3).

The calibration relating the photodiode output to the membrane displacement is obtained in a two-step process illustrated by the formula $\frac{\partial V_{1064}}{\partial x} = \left(\frac{\partial V_{1064}}{\partial f}\right)\left(\frac{\partial f}{\partial x}\right)$, where V_{1064} is the photodiode signal after the amplifier, x is the membrane position and f is the laser frequency.

The first step is to measure $\partial V_{1064}/\partial f$ by monitoring V_{1064} on a lock-in amplifier while modulating the laser frequency by a precise amount using an AOM. This step must be carried out whenever x_0, Δ or P is changed.

The second step is to determine $\partial f/\partial x$. In experiments using the 'usual' geometry illustrated in Fig. 1a this quantity is given simply by $\partial f/\partial x = c/\lambda L$ and does not need to be measured. However, for the dispersive coupling used in our experiments, $\partial f/\partial x$ is not immediately known: it varies with the position of the membrane in the cavity, x_0, corresponding to the slope of the curves in Fig. 1e. Therefore we must measure it, using a process illustrated by the formula $\frac{\partial f}{\partial x} = \left(\frac{\partial V_{1550}}{\partial x}\right)\left(\frac{\partial V_{1550}}{\partial V_{\mathrm{PZT}}}\right)^{-1}\left(\frac{\partial V_{1064}}{\partial V_{\mathrm{PZT}}}\right)\left(\frac{\partial V_{1064}}{\partial f}\right)^{-1}$. This quantity depends only on x_0 and is independent of Δ and P.

The first two steps in measuring $\partial f/\partial x$ involve a diode laser with wavelength 1,550 nm, for which the cavity finesse is ~1 and the transmitted and reflected intensities are sinusoidal functions of the membrane position. While driving the membrane through multiple free spectral ranges (using the piezo beneath the membrane), we measure the peak-to-peak change in the transmitted 1,550-nm photodiode signal, $V_{1550, \mathrm{P-P}}$. The formula $\left(\frac{\partial V_{1550}}{\partial x}\right) = \frac{\pi}{2}\frac{V_{1550, \mathrm{P-P}}}{\lambda/4}$ gives the maximum value of $\partial V_{1550}/\partial x$ over all x_0.

Then we measure $\partial V_{1550}/\partial V_{\mathrm{PZT}}$, the response of the transmitted 1,550-nm signal to a small driving voltage with amplitude V_0 applied to the piezo at a frequency several kilohertz above the fundamental membrane resonance, where the piezo's response is fairly independent of frequency. While driving the membrane, we change x_0 to maximize the modulation of the 1,550-nm signal, ensuring the 1,550-nm signal is described by $\partial V_{1550}/\partial x$ as measured above.

Finally, to measure $\partial V_{1064}/\partial V_{\mathrm{PZT}}$ and $\partial V_{1064}/\partial f$ we switch off the 1,550-nm laser, position the membrane at the desired x_0, and lock the 1,064-nm laser to the cavity with an arbitrary detuning (Δ) and power (P). Then we observe the change in V_{1064} while alternately driving the membrane with V_0 and modulating the laser frequency with a depth f_{AOM}.

We estimate that this calibration is accurate to within a factor of 2. However, the Q extracted by fitting the membrane motion (as shown in Fig. 3) is accurate to roughly 1% (the statistical error of the fit). The temperature extracted from the Q factor ($T_{\mathrm{eff}}^{(Q)}$) will not be the effective noise temperature if, for example, non-thermal force noises are acting on the membrane. However, in such circumstances $T_{\mathrm{eff}}^{(Q)}$ will always be less than $T_{\mathrm{eff}}^{(x)}$ (the temperature extracted from the displacement calibration). The fact that we see $T_{\mathrm{eff}}^{(Q)}$ greater than $T_{\mathrm{eff}}^{(x)}$ (by a factor of roughly 2) implies that the most likely reason behind the discrepancy is the imperfect calibration of the displacement signal.